

A Rationale for the Observed Non-Linearity in Pressure Tube Creep Sag with Time in Service

P.J. Sedran¹

¹ Fuel Channel Consultant – RESD Inc.
paulsedran@sympatico.ca

Abstract

In 2012, a paper was presented at the CNS SGC Conference which included an explanation for measured non-linear trends in Pressure Tube (PT) creep sag. The section of the 2012 paper covering this topic was revised and is presented as the main subject of this paper. The practical applications for the prediction of long-term Fuel Channel (FC) creep sag include the analysis of Calandria Tube – Liquid Injection Nozzle (CT-LIN) contact, and fuel passage and PT replacement assessments.

The current practice for predicting FC creep sag in life cycle management applications is to use a linear model for creep sag versus time in service. However, PT sag measurements from the Point Lepreau Generating Station (PLGS) and Gentilly-2 (G-2) have displayed a non-linear trend with a creep sag rate that is decreasing with time in service.

As an example, for PT F06 in PLGS, a 60% reduction in the nominal creep sag rate was observed for measurements taken 18 years apart. Subsequently, it was found that a 56% reduction in the creep sag rate for F06 over 18 years could be attributed to a fundamental geometric property of the PT creep sag profile. In addition, a further 1.6% decrease in the creep sag rate of the CT over the same period could be attributed to bending stress reductions due to the deformation of the CT.

The resultant reduction in the PT creep sag rate for F06 was predicted to be 57.6%, closely matching the observed PT creep sag rate reduction of 60%. Therefore, this paper provides a rationale to explain the observed non-linear trends in PT creep sag, the use of which could benefit stations engaging in asset management as a means of FC life extension.

This paper presents a summary of the work performed to correlate the observed reductions in PT creep sag rate to the geometrical properties of the PT creep sag profile and the predicted bending stress reductions in the CT.

1. Introduction

The issue of CT-LIN contact, which gained significant attention through a COG workshop in 1990 [1], has long been recognized as a life-limiting factor for the CTs. The measurement and prediction of FC creep sag rates have been central to the analysis of CT-LIN contact. In recent assessments, CT-LIN time-to-contact predictions for the CANDU 6 reactors indicate a significant risk of contact should the reactors operate beyond 210 kEFPH (kilo Effective Full Power Hours)

In reactors that have been refurbished, (Bruce Units 1 and 2, Point Lepreau, and Wolsong Unit 1), or are planning refurbishment by 210 kEFPH, CT-LIN contact will not be an issue for many years. However, for stations that are planning asset management strategies in order to operate beyond 210,000 EFPH, FC creep sag rates will factor into the remaining life of the FCs. For these stations, (Bruce 3 - 8 and Darlington) a number of refinements to the overall strategy for predicting CT-LIN time-to-contact have been developed. The refinements included the development of a non-linear empirical CT creep sag model. To justify the model, an explanation for the model's prediction of a decreasing creep sag rate with time in service is proposed in this paper, the contents of which are as follows:

Section 2 provides PT creep sag data for PLGS and G-2.

Section 3 provides a description of the geometric relationship between the rate of PT creep sag and the rate of creep-induced elongation of the arc length at the bottom of the PT.

Section 4 describes the acquisition of full-length CT inner diameter and curvature profiles from in-service PT inspection measurements in a selected channel in PLGS.

In Section 5, a comparative bending stress analysis for a pristine and a deformed CT is presented. The rationale for the analysis was based on the idea that possible bending stress reductions in the CT could result in decreasing FC creep sag rates with time in service.

A discussion of results is presented in Section 6.

Conclusions and Recommendations are provided in Sections 7 and 8.

References and Acknowledgements are found in Sections 9 and 10.

2. PT Creep Sag Data

Figure 1 presents a plot of maximum PT sag, (roughly at the centerline of the reactor) versus time in service for PLGS and for G-2. The data, which covers all of the PT sag measurements in the two reactors, are consistent with data used in the FC life cycle management documents for PLGS [2] and G-2 [3]. The PLGS data are plotted in Figure 1 in red. The red line is a power function regression for PT sag versus time in-service for PLGS. Similarly, the G-2 data and power function regression are shown in blue in Figure 1.

The PT sag data of Figure 1 was used to calculate nominal (not accounting for a 1 mm measurement accuracy in sag) PT creep sag rates. PT creep sag rate measurements for PLGS are presented in Figure 2. In the figure, a best fit line is plotted with the complete data set for PLGS. The red line in the figure represents a trend line for the PT in FC F06.

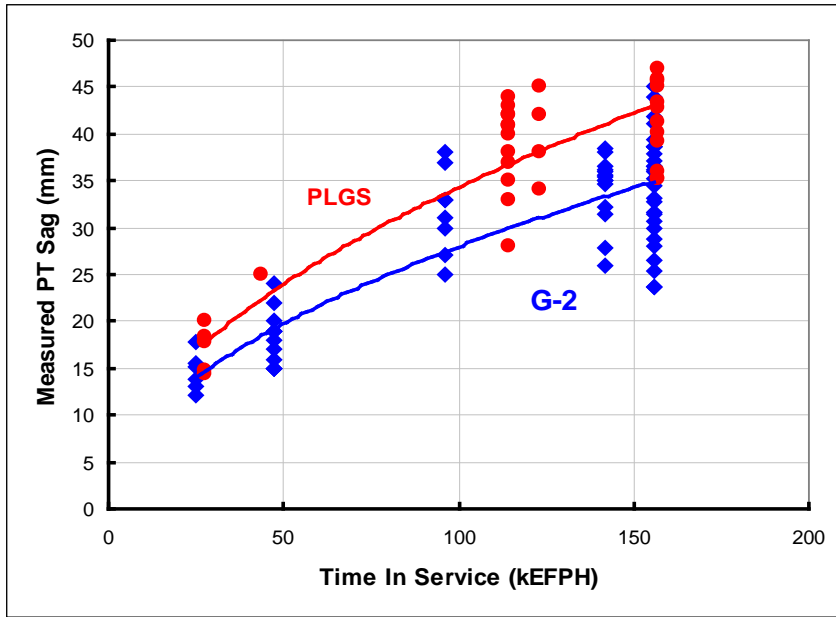


Figure 1 – PT Nominal Sag Data (at Peak Sag Locations) with Regression Lines for PLGS and G-2

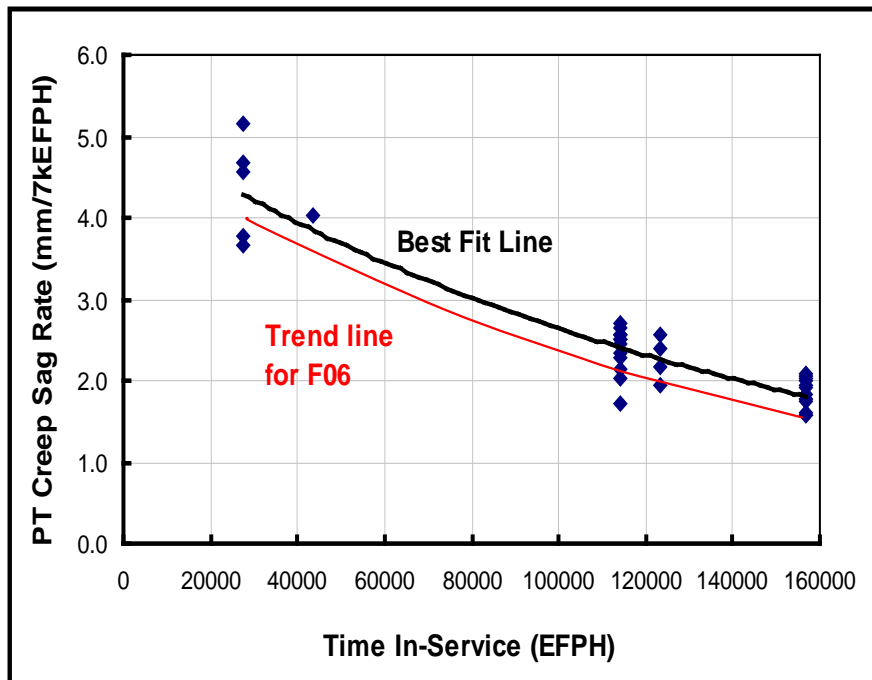


Figure 2 – PT Creep Sag Rates Versus Time In Service for PLGS

Based on Figure 2, the nominal PT sag rate for F06 has decreased from 4.0 mm/7 KEFPH at 27 KEFPH to 1.6 mm/7 KEFPH at 157, a decrease to 40% of the value at 27 KEFPH, which represents a reduction of 60% in the creep sag rate over the time period in question.

The implications of non-linear PT creep sag for the accuracy of creep sag predictions are illustrated in Figure 3. In the figure, MP (Measured to Predicted) ratio for PT sag is plotted versus time in-service. The predicted value of PT sag for each MP ratio data point in Figure 3 was generated using the CDEPTH code [4]. The trend is for MP ratio to start off around 1.0 early in the life of the reactor and then to decline with time in service. This trend is consistent with the non-linearity in PT sag observed in Figure 1. The linear sag deformation predictions are representative of the PT sag measurements early in the life of the reactor, but with increasing time in service, MP ratio decreases because the creep sag predictions of the linear model are increasingly different than the creep sag measurements, which follow a non-linear trend.

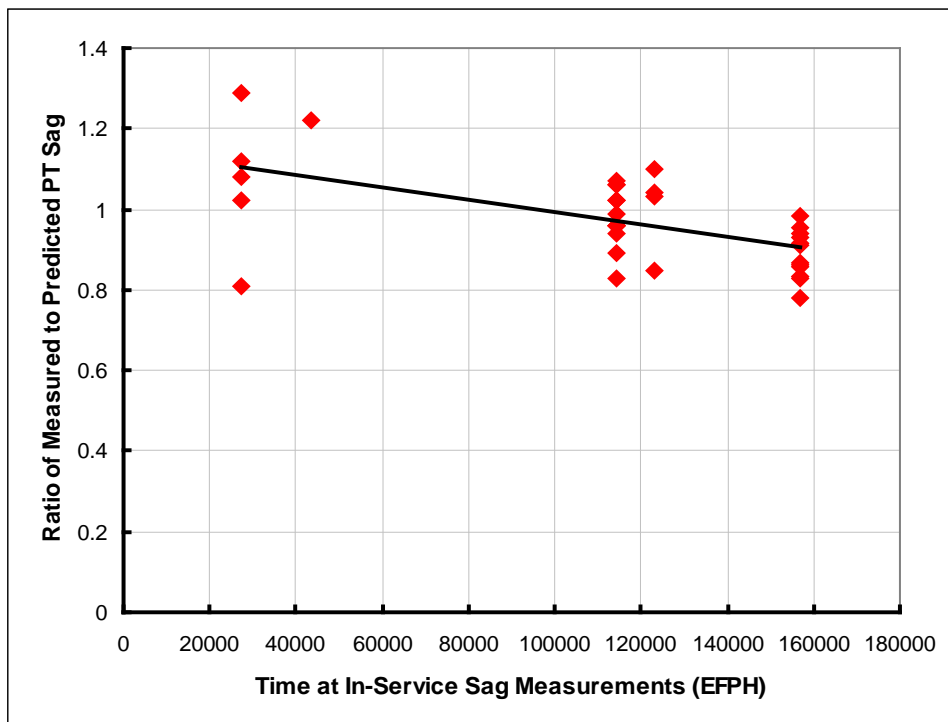


Figure 3 – Plot of MP Ratio for PT Sag in PLGS

3. Relationship between PT Creep Sag Deflection Rate and the Rate of Creep Induced Elongation of the Bottom of the PT.

In various analyses, for all CANDU stations, PT creep sag has been modelled as being linear with time in-service. The linear models do seem to fit the various data sets reasonably well and are conservative.

In previous assessments of CT-LIN contact, the CDEPTH code [4] was used to compute PT and CT creep sag, and there was no need to examine the fundamental geometry involved in the deformation of the PT. However, the examination of the fundamental geometry of PT deformation was undertaken in the attempt to explain the trends seen in Figures 1 and 2.

The thought process regarding the geometry of PT deformation proceeded as follows:

1. The bending of the PT under weight-loading produces tensile stresses at the bottom of the PT that result in local creep elongation at the bottom of the PT. Essentially, the arc length of a line on the outside surface at the bottom of the PT (PT arc length) will

increase with time.

2. Assuming that bending stress and fast neutron flux are constant with time in service and ignoring reductions in creep rate with neutron fluence, it is expected that the creep-induced elongation of the PT arc length will be constant with time in service.
3. However, the PT creep sag rate is seen to be decreasing with time in service. Is there a simple geometric argument to explain how the elongation rate of the PT arc length could be constant while the creep sag rate is decreasing with time in service?

Point 3, above, suggested the following relationship:

$$dy/dt = (dy/ds) (ds/dt) \tag{1}$$

Where dy/dt is the rate of creep sag, dy/ds is the rate of change in creep sag with arc length, and ds/dt is the rate of change in arc length. As indicated previously, ds/dt is assumed to be constant. If it could be shown that dy/ds reduces with time in service, with ds/dt , due to creep deformation, being constant, then dy/dt would also decrease with time in-service, as indicated in Figures 1 and 2. Note that y is the sag deflection of the bottom of the PT, i.e., the vertical distance of a point on the bottom of the deformed PT from the same point on a straight and horizontal PT. Figure 4 depicts the PT sag profile for F06 and illustrates the differentials dx , dy , and ds .

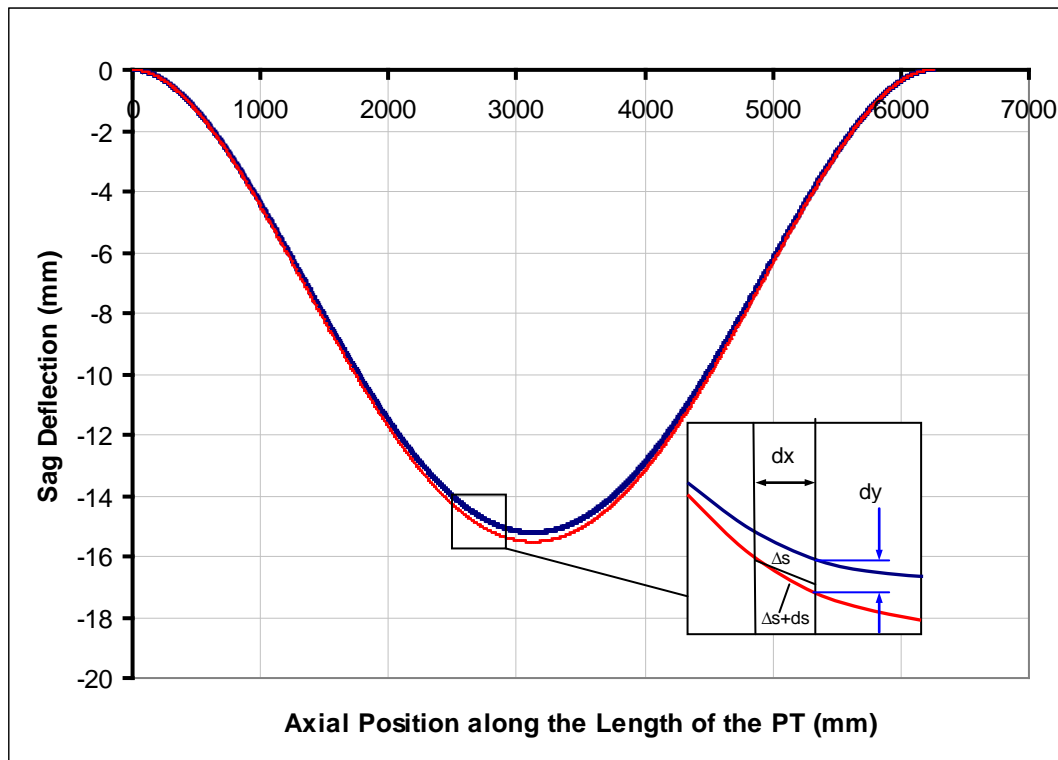


Figure 4 – PT Sag Profile for F06 with Illustrations for dx , dy , and ds

The blue line depicts the creep sag profile at 27 KEFPH and the red line represents the profile with an increment in sag of dy at a given position over a time step dt . Note that x is the axial coordinate. Over the interval dx , the length of the sag profile at 27 KEFPH is Δs . With creep deformation of the PT under bending stresses, the arc length of the sag profile from x to $x+dx$ increases by the increment ds , which results in dy at $x+dx$, all over the time step dt .

In order to study the variation in dy/ds for PT F06 at different times in service, finite difference computations of the PT arc length at 0, 27, and 157 KEFPH were performed in EXCEL. The PT

sag profile used in the computation of the PT arc length was that for a fixed-fixed beam under uniform lateral loading:

$$y(x) = w x^2 (L - x)^2 / 24 EI \quad (2)$$

Where $y(x)$ is the sag deflection, w is the load per unit length of the beam, x is the distance along the length of the beam, L is the length of the beam, E is the beam elastic modulus, and I is the area moment of inertia of the cross-section of the beam.

For each of the three cases, a small increment in sag was applied to the sag profile and a numerical approximation for dy/ds was obtained.

A summary of the PT arc length computations is presented in Table 1. The 0 KEFPH sag profile case represents the sag of the PT under static loading. The sag profiles for 27 and 157 KEFPH represent the measured creep sag profiles for PT F06. The sag and arc length increments, dy and ds , are presented with the computed values of dy/ds in Table 1.

Table 1 – Computation of dy/ds for PT F06 at Different Times

Time (KEFPH)	y (mm)	dy (mm)	S (mm)	ds (mm)	dy/ds (mm/mm)
0	1.65	1.93	6250.00106	0.003937	490.06
27	15.21	0.89	6250.09030	0.010936	81.83
157	35.08	0.72	6250.48011	0.019795	36.16

Note that S is the arc length for the entire PT, computed for the PT prior to the application of sag increment, dy , which applies to the centre of the channel.

Table 1 indicates that there is a rapid decrease in dy/ds with increasing PT sag. For a constant rate of PT arc length elongation, the PT sag rate would decrease with time.

Using dy/ds values from Table 1, dy/ds at 157 KEFPH was calculated to be $(36.16 \div 81.83)$ or 44.2% of that at 27 KEFPH. From Equation 1, assuming a constant ds/dt over time, dy/dt at 157 KEFPH would also be 44.2% of that at 27 KEFPH. The 44.2 % value computed from Table 1 compares reasonably well with the 40% value obtained for F06 in Section 2. .

In an attempt to reduce the predicted 44.2% creep sag rate ratio to a value closer to 40%, it was postulated that in-service induced deformation of the CT could reduce bending stresses and, therefore, the FC creep sag rate. An investigation of the affects of CT deformation on bending stress is summarized in Sections 4 and 5.

4. In-Service CT Deformation – Curvature and Inner Diameter Profiles

An example of the deformation of the CT, resulting from CT curvature, due to creep sag, combined with local deformation of the CT cross-sections, is presented below. The example is for the CT of Fuel Channel F06 in PLGS, which was inspected in 2004 at 157 KEFPH.

From the inspection of F06, in 2004, PT sag and curvature measurements were obtained. The PT sag and curvature profiles are given in Figure 5, which was reproduced from [5]. The PT sag data of Figure 5 was used to generate a corresponding CT sag profile.

In addition, PT gauging data from the 2004 inspection were combined with PT-CT gap profiles to generate an estimated CT inner diameter profile, depicted in Figure 6, from Reference [6].

Although the PT-CT gap profile used to generate the CT inner diameter profile was examined and appeared to be reasonable, the gap profile was not subject to quality assurance verification.

Therefore, until the PT-CT gap data is verified, the CT inner diameter profile presented in Figure 6 should be treated as preliminary.

The CT profile of Figure 6 indicates that there are local areas of diametral expansion of the CT at the spacer locations. The expansions are in the vertical direction only, and induce ovality in the CT, such that at the spacer location, the vertical diameter of the CT exceeds the horizontal diameter. The spacers are designed to support the weight of the fuel channel, and in turn are supported by the CT. The local deformation of the CT at the spacer locations, depicted in Figure 6, results from the high contact stresses that develop in the CT from spacer contact loading. Both curvature due to sag and CT diametral expansion were thought to stiffen the CT.

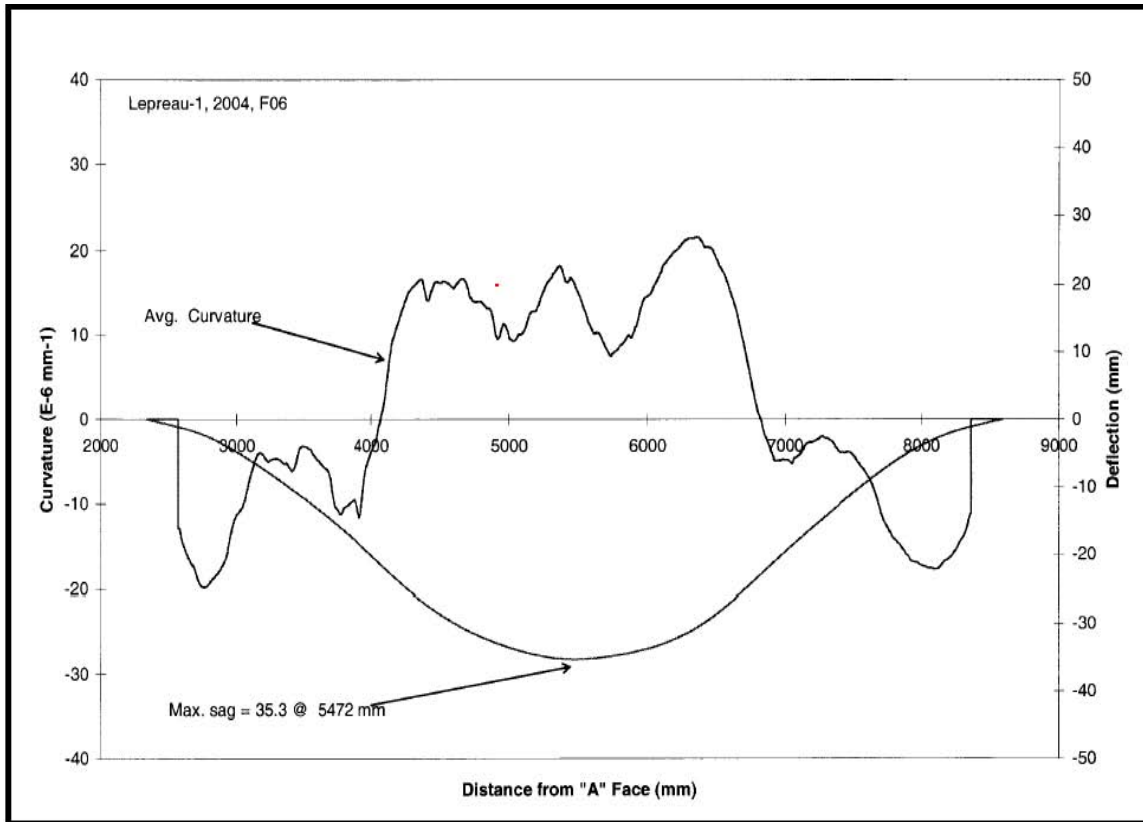


Figure 5 – PT Sag and Curvature for PLGS F06 at 157 keFPH

Figure from 87-31100-PIP-003, was provided by T. Langlais, NB Power Nuclear. The A Face is the East inspection face for the reactor for the 2004 Fuel Channel Inspection. The PT sag profile measurements are nominal values. For assessments, measurement error of plus or minus 1 mm on sag measurements are customary. The peaks in PT curvature represent local minimum radii of curvature of the PT due to bending of the PT at spacer locations.

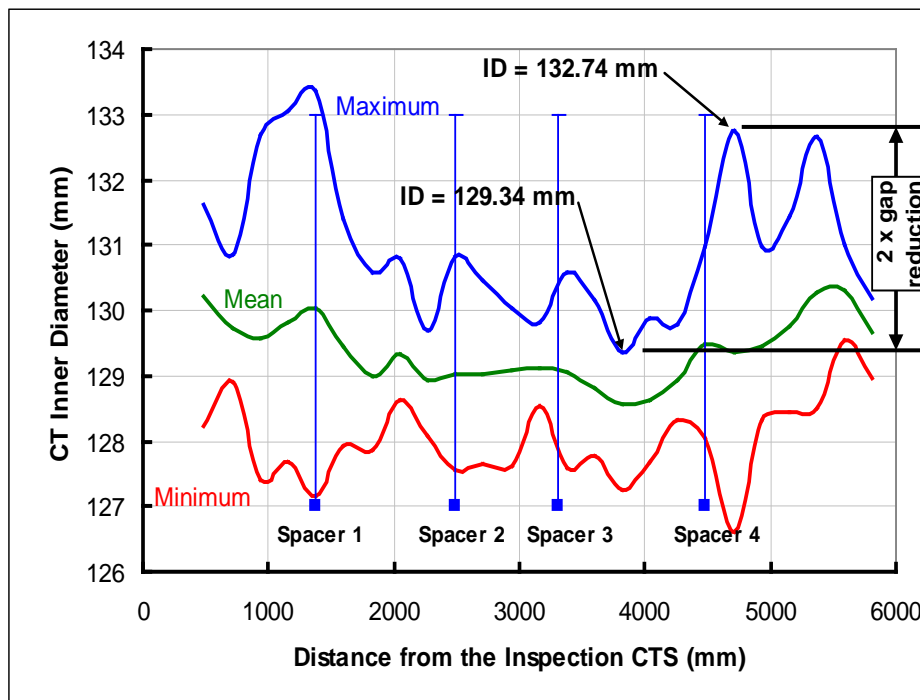


Figure 6 - Inner Diameter Profiles for the CT of F06 in PLGS at 157 KEFPH

CTS stands for Calandria Tube Sheet. The red line represents minimum diameter values at each section. Mean and maximum diameter values for each section are plotted in green and blue, respectively. The nominal inside diameter of the CT is 129 mm. At various sections of the CT, deformation has altered the section properties of the CT. The stress distribution at these sections deviates from that for a circular CT. The raw inspection data was provided by NB Power Nuclear staff.

5. Comparative Stress Analysis for a Pristine and a Deformed CT

When indications of non-linear creep sag of the PTs appeared, a physical explanation was sought for why the creep sag of the PT would decrease with time in-service, which led to the investigations summarized in this section.

In CDEPTH, the elements of the PT and CT models are modelled as straight beams, conventionally with a uniform cross-section. Intuitively, because the deformations of the PT and CT seem to be relatively small, the use of straight beam models for the PT and CT has continued in CDEPTH has not been questioned. However, in recent years, fairly significant PT and CT deformations have been detected. Early speculation was that the diametral deformation of the CT and curvature of the CT would increase its stiffness and would reduce the rate of creep sag with time in-service, explaining the trend seen in Figure 1.

Following that line of thought, a comparative stress analysis was performed for the pristine CT in F06 in PLGS and for the deformed CT at 157 KEFPH. . The pristine CT was assumed to be straight and cylindrical, as in the CT stress calculation for CDEPTH. The deformed CT was assigned local curvatures due to the creep sag and vertical and horizontal outer diameters based on the results of the inspection at 157 KEFPH, shown in Figures 5 and 6. For both cases, σ/M was calculated for sections of the CT at discrete axial positions along the length of the CT, where σ is the axial stress due to bending and M is the applied bending moment. For the pristine CT, σ/M was calculated using the flexure formula for straight beams. For the deformed CT, σ/M was calculated using the following closed form solution for beams of constant curvature,

from [7]:

$$\sigma = \frac{My}{Ae(R - y)} \tag{3}$$

Where y is the distance from the neutral axis for the given section, A is the cross-sectional area of the section of the CT, e is the eccentricity of the section (the distance between the neutral axis and the geometric centroid of the section), and R is the radius of curvature for the section. The results of the comparative stress analysis are presented in Figure 7.

In Figure 7, the ratio of the maximum σ/M value at a given section for the deformed CT to that for the same section in the pristine CT is plotted for various sections of the CT. In this case, the maximum σ/M ratio is plotted for the central 2 m length of the CT. As seen in the figure, the reduction in bending stress in the deformed CT, relative to the pristine CT, is not significant. Over the central 2 m segment of the deformed CT, the average σ/M ratio is 0.984. One would expect a reduction of 1.6% in bending stress in the central segment of the deformed CT that would lead to a reduction in the CT creep sag rate, compared to that in the pristine CT.

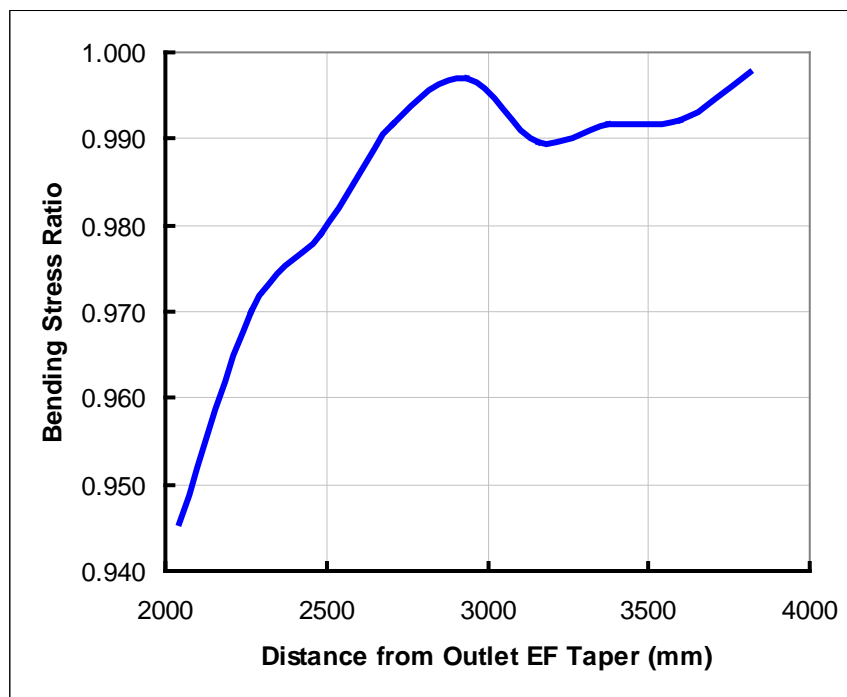


Figure 7 – Plot of Bending Stress Ratio for the Deformed and Pristine CT from F06 in PLGS versus Distance from the Outlet EF Taper

Note: EF stands for End Fitting. .

6. Discussion of Results

At this point, the results given in Sections 3 and 5 can be combined as follows:

Recalling that $dy/dt = (dy/ds) (ds/dt)$, from Section 3, dy/ds for the PT at 157 KEFPH was found to be 44.2% of dy/ds at 27 KEFPH.

Also, from Section 5, it was predicted that the bending stress per unit bending moment in the CT would be reduced by 1.6% in the deformed PT compared to the pristine CT. Assuming no significant change in bending moments, this would result in a 1.6% reduction in ds/dt in the deformed CT at 157 KEFPH compared to that of the pristine CT. The bending stress at 157 KEFPH would then be 98.4% of that in the pristine CT. For the purposes of this paper, it is assumed that reductions in ds/dt for the CT would be similar to those for the PT.

Considering the influence of the reduction in dy/ds and in ds/dt for the PT over the interval from 27 KEFPH to 157 KEFPH, the PT creep sag rate at 157 KEFPH can be expressed as a fraction of the creep sag rate at 27 KEFPH as follows:

$$dy/dt (157 \text{ KEFPH}) = (0.442) dy/ds \bullet (0.984) ds/dt (27 \text{ KEFPH}) = 0.435 dy/dt (27 \text{ KEFPH})$$

Therefore, it is predicted that the creep sag rate for the PT at 157 KEFPH would be 43.5 % of the creep sag rate at 27 KEFPH. In Section 2, the observed nominal creep sag rate for PT F06 at 157 KEFPH was determined to be 40.0% of the creep sag rate at 27 KEFPH. The predicted decrease in the rate of PT creep sag with time in service for F06, based on the geometry of PT deformation and (to a lesser degree) on the evolution of CT bending stress, matches the observed trend for PT F06.

7. Conclusions

1. PT sag measurements from the inspection of PLGS and G-2 indicate that PT and, therefore, CT creep sag are non-linear functions of time in service.
2. In the case of F06 in PLGS, the nominal PT creep sag rate at 157 KEFPH was found to be 40.0% of that at 27 KEFPH.
3. For a constant PT arc length elongation rate, PT sag profile geometry dictates that the PT sag rate will decrease with increasing sag. It was predicted that because of this geometric property, the creep sag rate for F06 at 157 KEFPH would be 44.2% of that at 27 KEFPH.
4. Based on a simple analysis of the geometry of PT deformation and CT bending stresses, it was predicted that the PT creep sag rate for F06 at 157 KEFPH would be 43.5% of that at 27 KEFPH, compared with the observed 40% value. Therefore, the non-linear trend for PT creep sag with time in service in Figures 1 and 2 can be explained on the basis of the geometry of PT deformation (with a small contribution from changes in CT bending stress).

8. Recommendations

Future predictions of FC creep sag should be conducted using non-linear models for creep sag with time in service. .

9. References

- [1] S.S. Dua, W. Clendening, "Calandria Tube Sag and Contact with Mechanisms Workshop", Oakville, Ontario, Canada, February 19, 1990.
- [2] A. Crandell, "Technical Basis of the Fuel Channel Ageing and Life Cycle Management Plan for

Point Lepreau NGS”, 87-31100-TD-004, Revision 0, June, 2005.

- [3] P.J. Sedran, “Fuel Channel Ageing and Life Cycle Management Plan”, Gentilly-2, 66-31100-TD-001, Revision 0. May 31, 2004.
- [4] R.G. Sauve, N. Badie, G. Morandin, “Creep Response of Fuel Channels in CANDU Nuclear Reactors: Computer Code CDEPTH, Version 8.2”, Kinectrics Report: 8745-001-RA-0001-R00, October, 2001.
- [5] A. Lepage, T. Edwards, T. Krause, G. Longhurst, S. Donahue, D. Kalenchuk, K. Sonnenburg, T. Joulín, and A. Martin, “Fuel Channel Periodic Inspection: 2004, May – Final Report”, Point Lepreau – 1, 87-31100-PIP-003, September, 2004.
- [6] P.J. Sedran, B. Rankin, “The Use of OPEX (in the Form of Inspection Data) to Obtain Unanticipated Calandria Tube Ovality Measurements”, 9th CNS International Conference on CANDU® Maintenance, Toronto, Ontario, Canada, December 4-6, 2011
- [7] J.E. Shigley, “Mechanical Engineering Design”, Third Edition, McGraw-Hill Book Company, Toronto, 1977.

10. Acknowledgements

Thanks are due to Bill Rankin, NB Power Nuclear, PLGS and to Michel Cantin, Hydro-Québec - Centrale Gentilly-2 for permission to use data from various inspections (Figure 1).